J. Chem. Sci. Vol. 128, No. 9, September 2016, pp. 1385–1393.
DOI 10.1007/s12039-016-1137-6

Poly[tetraaquatriglutaratodicerium(III) decahydrate], a novel luminescent metal-organic framework possessing hydrophilic hexagonal channels

REMYA M NAIR[a], M R SUDARSANAKUMAR[a,b,*], S SUMA[c], M R PRATHAPACHANDRA KURUP[d] and P K SUDHADEVI ANTHARJANAM[e]

[a]Present address: Department of Chemistry, Mahatma Gandhi College, Thiruvananthapuram, Kerala, 695 004 India
[b]VTM NSS College, Dhanuvachapuram, Thiruvananthapuram, Kerala, 695 503 India
[c]Department of Chemistry, S N College, Chempazhanthy, Thiruvananthapuram, Kerala, 695 587 India
[d]Department of Applied Chemistry, Cochin University of Science and Technology, Kochi, Kerala, 682 022, India
[e]XRD Lab, SAIF, IIT-Madras Chennai, Tamilnadu, 600 036 India
e-mail: sudarsanmr@gmail.com

MS received 22 December 2015; revised 21 May 2016; accepted 2 July 2016

Abstract. A novel 2D metal–organic framework poly[tetraaquatriglutaratodicerium(III) decahydrate] with an open framework structure has been successfully grown by single gel diffusion technique. Sodium metasilicate was used for gel preparation. The structure was determined by single crystal X-ray diffraction. The compound crystallizes in orthorhombic space group *Pnma* and possesses a structure consisting of $[CeO_{10}]$ polyhedra and H_2O molecules with hydrophilic hexagonal channels. The crystals were further characterized by elemental analysis, FT-IR and UV-Visible spectroscopy, powder X-ray diffraction and thermogravimetry. The luminescent property and magnetic susceptibility of the complex were also investigated.

Keywords. Metal-organic framework; gel method; 2D complex; porous architecture; hydrophilic channels; luminescence.

1. Introduction

Studies on metal–organic framework materials have become a fascinating topic over the past decades owing to their interesting properties and intriguing structural motifs. Metal–organic frameworks (MOFs) have potential applications in many fields such as gas storage, adsorption, shape selective seperation, catalysis, ion-exchange, non-linear optics and so on.[1–6] Rare earth elements have considerable application in technological fields.[7–9] Owing to the unique nature of lanthanide ions such as their large radius, high and variable coordination numbers, they have been employed for the construction of MOFs having excellent magnetic and luminescent properties.[10–13] However, it is still a great challenge to synthesise lanthanide complexes of desired topology due to a number of challenging factors. Hence, judicious and rational choice of organic ligands is a crucial element in the synthesis and design of lanthanide MOFs. For the construction of these MOFs, flexible dicarboxylates with $–CH_2–$ spacer are usually selected. Unlike rigid aromatic dicarboxylates, they can bend and rotate freely when coordinated to metal centres, causing structural pecularities and producing unique structures. Glutaric acid, the next higher homologue of succinic acid is an excellent flexible ligand and can exhibit abundant coordination modes thus giving rise to extended structures with dimensionalities ranging from 1D to 3D.[14–16] It was well-established that lanthanides have a strong tendency to coordinate to O-donor atoms to form lanthanide-carboxylate coordination polymers.[17] Moreover, crystallization of metal glutarates by gel method is limited in the literature.[18]

Taking into account all these factors, we have grown a novel 2D porous lanthanide MOF, poly[tetraaquatriglutaratodicerium(III) decahydrate] $([Ce_2(glu)_3(H_2O)_4]\cdot 10H_2O)_n$ possessing hydrophilic hexagonal channels. To the best of our knowledge, this is the first report of the title compound. Crystal structure of a related compound *viz.,* poly([tetraaqua-μ_4-glutarato-cerium(III)]chloride dihydrate) was reported[19] which is an ionic 2D open framework compound with Cl^- as the counter ion but our compound possesses a different structure compared to the reported one. The crystals grown were

*For correspondence

further characterized by elemental analysis, FT-IR and UV-Visible spectroscopy, thermogravimetry, powder X-ray and single crystal X-ray diffraction studies. The luminescent property and magnetic susceptibility of the complex were also investigated.

2. Experimental

2.1 *Materials and methods*

Glutaric acid (CDH) and cerium nitrate (CDH) were of AR grade and used without further purification. The carbon and hydrogen content present in the grown crystals were found using Elementer Vario–EL 111 CHNS analyzer. The FT-IR spectrum was recorded using KBr pellets on a Thermo Nicolet, Avatar 370 spectrometer in the range 4000–400 cm^{-1}. Powder X-ray diffraction studies were carried out using a Bruker AXS D8 advance XRD with Cu Kα radiation (λ = 1.54056 Å). The solid state optical absorption spectrum was recorded using Varian Cary 5000 UV-VisibleNIR spectrometer in the range 200–1200 nm. The thermal analysis of the crystals was carried out using a Perkin Elmer Diamond TG/DTG analyzer instrument at a heating rate of 10°C/min in nitrogen atmosphere. The photoluminescence spectra of the ligand and the complex were recorded using JY Horiba PL meter at room temperature. Magnetic susceptibility measurement of the sample was carried out using Sherwood Scientific MK-1 magnetic susceptibility meter.

2.2 *Growth procedure of* $([Ce_2(glu)_3(H_2O)_4]\cdot 10H_2O)_n$

Single gel diffusion technique was used for growing quality crystals of $([Ce_2(glu)_3(H_2O)_4]\cdot 10H_2O)_n$.[20–22] Silica hydrogel prepared from an aqueous solution of sodium metasilicate (SMS) was employed for this purpose. A series of experiments were conducted for obtaining good quality crystals and the optimum conditions for crystal growth are as follows: [glutaric acid] = 1 M, [cerium nitrate] = 0.5 M, gel density = 1.04 g cm^{-3} and pH = 5.5. Anal. Calcd for $([Ce_2(glu)_3(H_2O)_4]\cdot 10H_2O)_n$: C, 19.50%; H, 4.98%. Found: C, 19.68%; H, 4.57%. FT-IR (KBr cm^{-1}) 3413b, 1540vs, 1417vs, 2970w, 1058m, 645s. Magnetic moment (μ, B.M.): 2.56.

2.3 *Single crystal X-ray diffraction analysis*

The single crystal X-ray diffraction studies were carried out using a Bruker AXS Kappa Apex2 CCD diffractometer at room temperature with graphite monochromated Mo Kα (λ = 0.71073 Å) radiation. The unit

Figure 1. Photograph of crystalline $([Ce_2(glu)_3(H_2O)_4]\cdot 10H_2O)_n$.

cell dimensions and intensity data were recorded at 293 K. The program SAINT/XPREP was used for data reduction and APEX2/SAINT for cell refinement.[23] The structure was solved by SIR92 and refined by full-matrix least squares on F^2 using SHELXL-97 computer programs.[24] All non-hydrogen atoms were refined with anisotropic thermal parameters. Carbon-bound H-atoms were placed in calculated positions and included in the refinement in the riding model approximation. The hydrogen atoms of the lattice water molecules could not be located in the difference Fourier map, and were not included in the structure. DIAMOND software version 3.1f was employed for structure plotting.[25]

3. Results and Discussion

3.1 *Crystal growth*

Transparent, good quality single crystals essential for single crystal X-ray diffraction studies appeared at the gel interface after 5 days. Fully grown crystals were carefully separated from the gel interface, washed several times with distilled water to remove gel impurities and finally dried. Figure 1 shows the photograph of crystalline $([Ce_2(glu)_3(H_2O)_4]\cdot 10H_2O)_n$.

3.2 *Powder X-ray diffraction studies*

Powder X-ray diffraction studies were carried out using a Bruker AXS D8 advance XRD with Cu Kα radiation ($\lambda = 1.54056$ Å). The crystalline nature of the complex was confirmed from the well defined Braggs peaks at specific 2θ angles. The phase purity of the bulk sample was determined by comparing the powder XRD pattern with the simulated one obtained from single crystal X-ray diffraction data using the Mercury software.[26] Experimental and simulated powder X-ray diffractograms are shown in Figure 2. As shown, the peak positions of the experimental pattern of the complex match well with the simulated one, confirming that the complex had been obtained as pure crystalline phase. Slight differences observed may be due to the preferred orientation of the powder sample.

3.3 *Crystal structure of* $([Ce_2(glu)_3(H_2O)_4]\cdot 10H_2O)_n$

X-ray single crystal analysis reveals that the title compound is a 2D metal–organic framework possessing hydrophilic hexagonal channels with interconnected $[CeO_{10}]$ polyhedra. The compound crystallizes in orthorhombic *Pnma* space group. The corresponding unit cell parameters are a = 8.75270(10) Å, b = 30.9753(5) Å, c = 13.0054(2) Å, $\alpha = \beta = \gamma = 90°$.

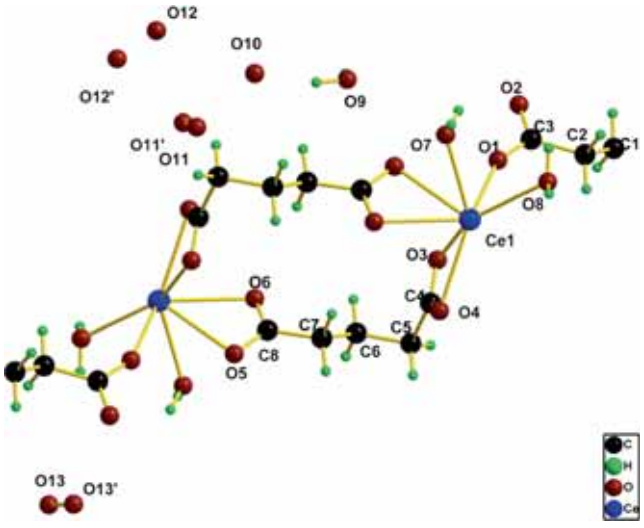

Figure 3. Asymmetric unit of $([Ce_2(glu)_3(H_2O)_4]\cdot 10H_2O)_n$.

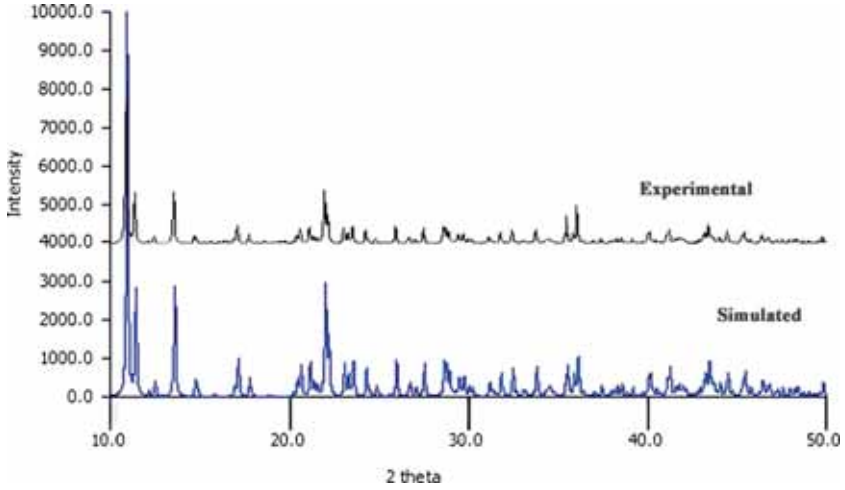

Figure 2. Experimental and simulated X-ray diffractogram of $([Ce_2(glu)_3(H_2O)_4]\cdot 10H_2O)_n$.

Table 1. Crystal data and structure refinement parameters of $([Ce_2(glu)_3(H_2O)_4]\cdot 10H_2O)_n$.

Parameters	$([Ce_2(glu)_3(H_2O)_4]\cdot 10H_2O)_n$
Empirical formula	$C_{15}H_{46}Ce_2O_{26}$
Formula weight (M)	922.76
Temperature (T) (K)	296(2)
Wavelength (Mo Kα) (Å)	0.71073
Crystal system	Orthorhombic
Space group	*Pnma*
Unit cell dimensions	a (Å) = 8.75270(10), $\alpha = 90°$
	b (Å) = 30.9753(5), $\beta = 90°$
	c (Å) = 13.0054(2), $\gamma = 90°$
Volume V (Å^3)	3525.99(9)
Z, Dcalc (ρ) (Mg/m3)	4, 1.708
Absorption Coefficietnt, μ (mm-1)	2.636
F(000)	1840
Crystal size (mm^3)	0.30 x 0.25 x 0.20
Colour, nature	colourless, block
θ Range for data collection (°)	2.52 to 25.00
Independent reflections (R_{int})	0.0744
Limiting indices	$-10 \leq h \leq 10$, $-23 \leq k \leq 36$, $-13 \leq l \leq 15$
Reflections collected/ unique	18903
Completeness to θ	99.9%
Absorption correction	Semi-empirical from equivalents
Max. and min. transmission	0.679 and 0.581
Refinement method	Full-matrix least squares on F^2
Data /restraints/parameters	3171 / 71 / 246
Goodness-of-fit on F^2	1.258
Final R indices [(I>2σ(I)]	$R_1 = 0.0446$, $wR_2 = 0.1024$
R indices (all data)	$R_1 = 0.0504$, $wR_2 = 0.1069$
Largest difference peak and hole (e Å^{-3})	1.235 and −1.870

$R_1 = \Sigma \| F_o | - | F_c \| / \Sigma | F_o |$: $wR_2 = [\Sigma w(F_o^2 - F_c^2)^2 / \Sigma w(F_o^2)^2]^{1/2}$

The asymmetric unit of $([Ce_2(glu)_3(H_2O)_4]\cdot 10H_2O)_n$ along with atom numbering scheme is shown in Figure 3. The crystallographic data along with details of structure solution refinements are given in Table 1 and some selected bond lengths and bond angles are presented in Table S1 (Supplementary Information). There is one crystallographically unique cerium atom, one and a half glutarate, two coordinated and five lattice water molecules in the asymmetric unit. Of the five lattice water molecules, three are disordered into several positions (O11, O12 and O13). The asymmetric unit excluding the lattice water molecules are shown in Figure S1 (Supplementary Information). The presence of these coordinated and lattice water molecules provides crystalline stability for the complex *via* a network of hydrogen bonding interactions.

The coordination environment of $([Ce_2(glu)_3(H_2O)_4]\cdot 10H_2O)_n$ is shown in Figure 4. As shown, each cerium atom is decacoordinated with respect to eight oxygen atoms from five different glutarate moieties and the remaining two are from coordinated water molecules to form a slightly distorted $[CeO_{10}]$ polyhedron while in the related reported structure,[19] cerium(III) ion shows a coordination number of nine defined by four water

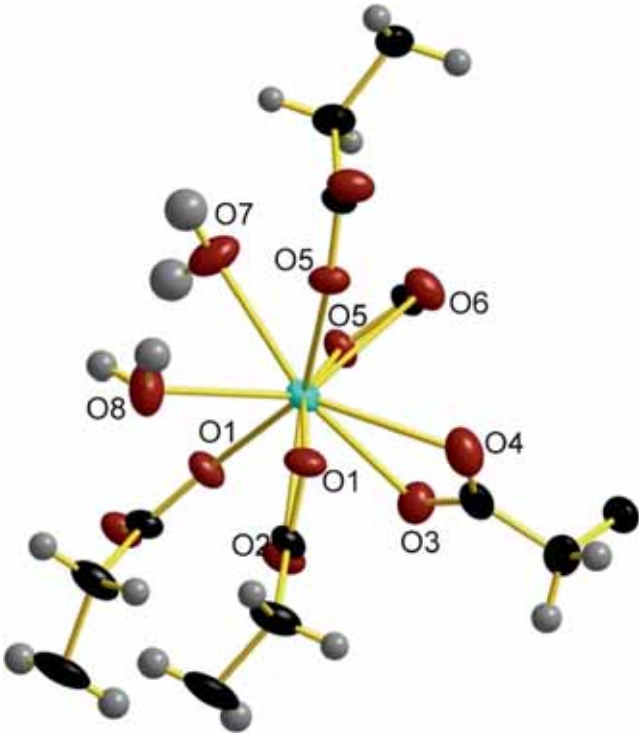

Figure 4. Coordination environment of $([Ce_2(glu)_3(H_2O)_4]\cdot 10H_2O)_n$.

oxygen atoms and five carboxylate oxygen atoms from glutarato ligands. In this complex, three of the carboxylate groups are coordinated to the metal ion in a typical bidentate mode and the remaining ones coordinate in a monodentate manner. Through the bidentate coordination, the compound gets chelated which further enhances the stability of the complex. The Ce–O bond lengths are in the range of 2.444(4) Å to 2.756(4) Å and the bond lengths of Ce–O7 and Ce–O8 are 2.611(5) and 2.555(5) Å, respectively. The Ce–O bond distances are comparable to those observed in other Ce(III) complexes except Ce–O1#6 = 2.729(4), symmetry code: #6 x+1/2,y,-z+1/2 and Ce–O5#3 = 2.756(4), symmetry code: #3 -x+1,-y+1,-z+1, which is a little longer than the literature value. However, the average value of these bond distances is consistent with the reported values for other Ce(III) complexes.[19,27] The carboxylate groups of the glutarate moiety exhibit two types of coordination mode in $([Ce_2(glu)_3(H_2O)_4]\cdot 10H_2O)_n$. In the first case, the carboxylate groups are found to coordinate tridentately on both ends of the molecule and adopt a μ_2–η^2, η^1 bridging mode and in the latter case, the carboxylate groups are found to coordinate tridentately on one side and bidentately on the other side. Thus, the carboxylate oxygens of the glutarate moiety can act both as bis-bridging and bis-chelating unit.

In this structure, the adjacent $[CeO_{10}]$ polyhedra are connected *via* bridging oxygen atoms (O1 and O5) of the carboxylate groups of glutarate and the bridging of the cerium centres by the glutarate oxygens results in the formation of O–Ce–O 1D polymeric chains (Figure 5). Within this 1D chain, Ce$\cdots$Ce non-bonding distance is found to be 4.3854(4) Å. These 1D chains are then interconnected by the pillaring glutarate units to form the 2D structure. The perspective view of the 2D structure along the crystallographic 'c' axis is shown in Figure 6. An importantant characteristic of this structure is the presence of hexagonal channels. Lattice water molecules are found to be entrapped in some of these channels which make them hydrophilic. The polyhedral design of the compound clearly presents these hexagonal channels (Figure 7). It was well-established that porous MOFs have potential applications in the field of gas storage and adsorption.[28,29]

The hydrogen bonding interactions are summarized in Table 2. Here, the lattice water molecule O9 acts

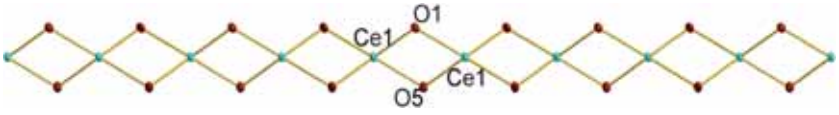

Figure 5. 1D polymeric chain formed by bridging oxygen atoms.

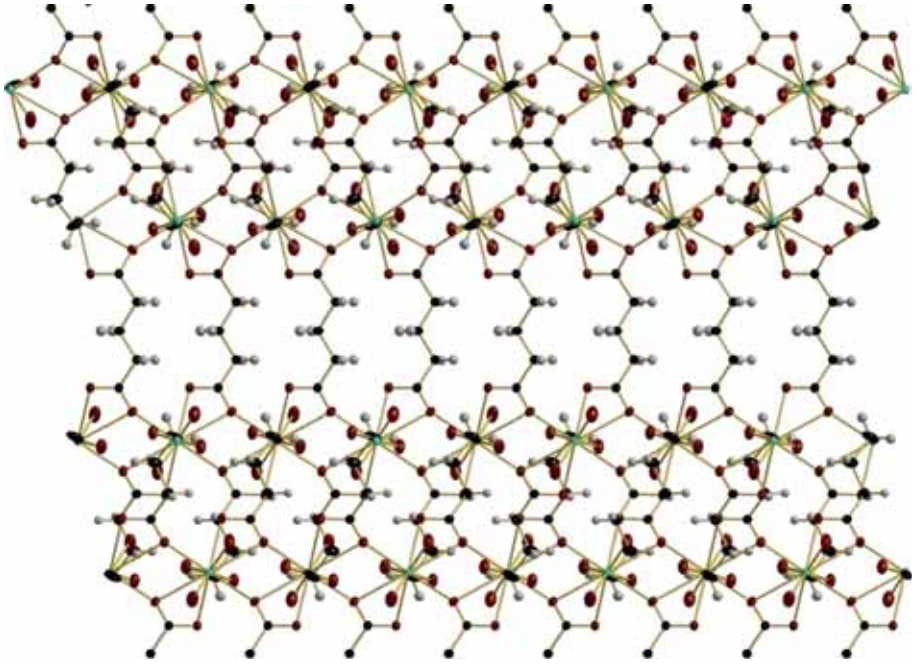

Figure 6. Perspective view of the 2D structure of $([Ce_2(glu)_3(H_2O)_4]\cdot 10H_2O)_n$ along 'c' axis. (Lattice water molecules are omitted for clarity).

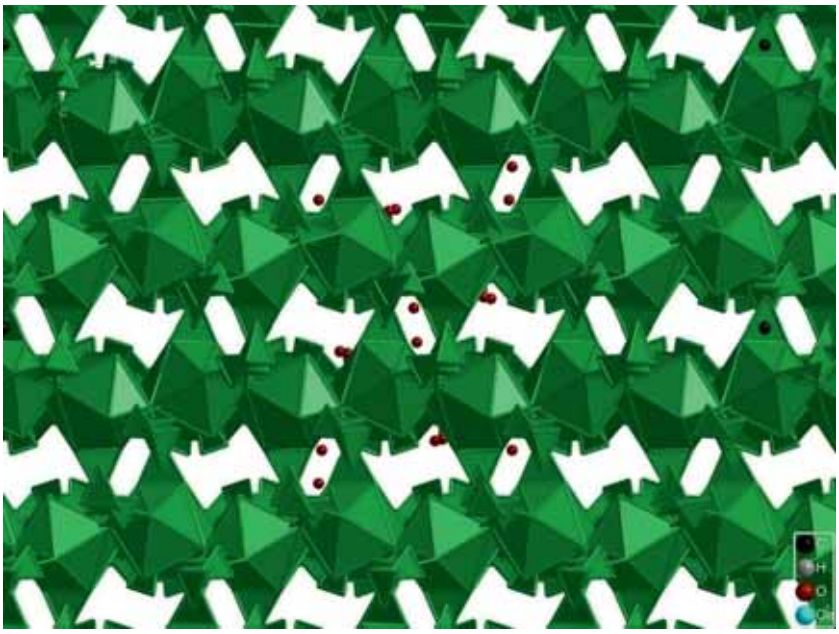

Figure 7. Polyhedral view of hydrophilic hexagonal channels in $([Ce_2(glu)_3(H_2O)_4]\cdot 10H_2O)_n$.

Table 2. Hydrogen bonds for $([Ce_2(glu)_3(H_2O)_4]\cdot 10H_2O)_n$.

D–H···A	**d(D–H) (Å)**	**d(H···A) (Å)**	**d(D···A) (Å)**	**<(DHA) (°)**
C(2)–H(2B)···O(2)#6	0.97	2.51	3.369(8)	148.2
O(8)–H(8A)···O(10)#7	0.89(2)	1.93(3)	2.798(12)	165(6)
O(8)–H(8B)···O(3)#6	0.89(2)	1.84(2)	2.723(7)	170(7)
O(7)–H(7C)···O(9)#7	0.904(15)	1.94(5)	2.769(7)	153(8)
O(9)–H(9A)···O(10)	0.90(2)	2.14(3)	2.999(15)	158(6)
O(9)–H(9B)···O(6)#8	0.90(2)	1.87(2)	2.760(7)	171(9)
O(7)–H(7D)···O(4)#2	0.91(2)	1.89(4)	2.766(7)	161(10)

Symmetry transformations used to generate equivalent atoms:
#1 x,-y+3/2,z #2 x-1/2,y,-z+1/2 #3 -x+1,-y+1,-z+1.
#4 -x+3/2,-y+1,z+1/2 #5 -x+3/2,-y+1,z-1/2 #6 x+1/2,y,-z+1/2.
#7 x,y,z-1 #8 x+1/2,y,-z+3/2.

as both donor and acceptor and is involved in hydrogen bonding to carboxylate oxygen atoms O6 and O7, respectively. Similarly the lattice water molecule O10 acts as acceptor and is hydrogen bonded to O9 and to hydrogen atom of one of the coordinated water molecules, O8. The other hydrogen atom of the coordinated water molecule O8 is bonded to carboxylate oxygen atom O3. Similarly, hydrogen atom of the coordinated water molecule O7 is bonded to carboxylate oxygen atom O4. The hydrogen bonds are also supplemented by C–H···O hydrogen bonding interaction between C2 carbon and carboxylate oxygen atom, O2. These observations indicate that the noncovalent interactions provide significant contribution to the stabilisation of the 2D framework. Figure 8 shows the hydrogen bonding in $([Ce_2(glu)_3(H_2O)_4]\cdot 10H_2O)_n$.

3.4 *FT-IR spectral studies*

FT-IR spectral studies were carried out to analyze the functional groups present in the complex and the resulting spectrum is shown in Figure S2 (Supplementary Information). The spectrum shows a broad band of OH stretching vibration of water molecules at 3413 cm^{-1}. The strong band at 1700 cm^{-1} attributed to ν(C=O) vibration of carboxylic acid group of the free ligand is absent in the spectrum of the complex indicating coordination of ligand to the metal through carboxylate group after deprotonation.[30] The asymmetric and symmetric stretching vibrations of the carboxylate group are observed at 1540 and 1417 cm^{-1}, respectively. A weak absorption band at 2970 cm^{-1} is attributed to ν(CH) vibration of CH_2 group.[31] Stretching vibration of

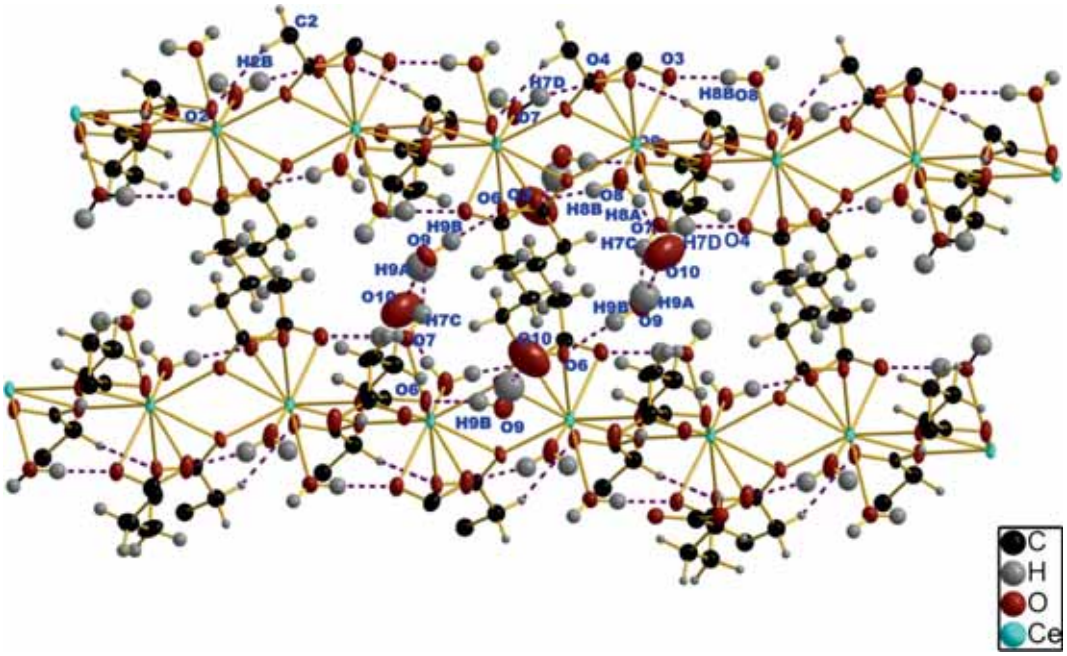

Figure 8. Hydrogen bonding interactions in $([Ce_2(glu)_3(H_2O)_4]\cdot 10H_2O)_n$.

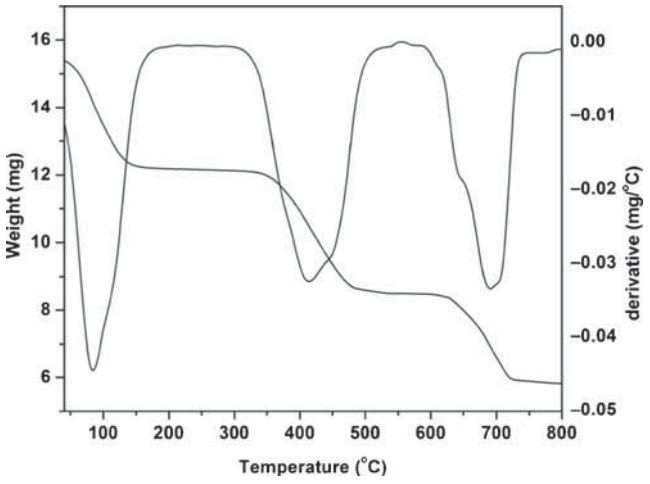

Figure 9. TG/DTG curve of $([Ce_2(glu)_3(H_2O)_4]\cdot 10H_2O)_n$.

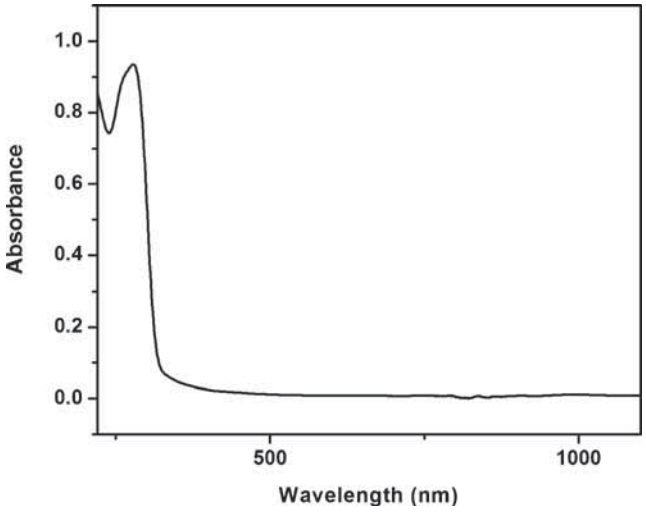

Figure 10. UV-Visible spectrum of $([Ce_2(glu)_3(H_2O)_4]\cdot 10H_2O)_n$.

C–C bond appears at 1058 cm^{-1}. The bending vibration of COO^- is observed at 645 cm^{-1}.

3.5 *Thermogravimetry*

The thermal decomposition behaviour of the crystals was investigated and the thermogram is shown in Figure 9. From the figure, it is clear that the compound decomposes in three stages. The first weight loss of 14.59% in the temperature range 70–230°C corresponds to the loss of water molecules (calculated: 14%). The next two stages correspond to the total removal of the organic ligand moiety with the formation of corresponding metal oxide as the final product. The observed and calculated mass losses are 57.21 and 56.78%, respectively.

3.6 *UV-Visible absorbtion studies*

The UV-Visible absorption spectrum is shown in Figure 10. The spectrum of Ce(III) is quite different as compared to other lanthanide compounds. The lowest energy transition of Ce(III) involves the promotion of an electron from 4f to the 5d orbitals. Since the ground and the excited states of this f^1 ion are spin doublets, all

transitions are spin-allowed. The corresponding absorptions appear in the UV region. The single absorption peak at 278 nm is due to the 4f-5d electronic transitions in Ce^{3+} ions. From the spectrum, it is clear that, the crystals are transparent in the entire visible region. Generally, Ce(III) complexes are colourless since the metal centred f-d transition gives rise to an absorption in the near UV region. The free acid is also colourless so upon coordination, the intraligand bands remain in the UV region.[32]

3.7 *Photoluminescence studies*

Lanthanide complexes play an important role in luminescence spectroscopy. The chemical structure and the tunability of the position of the strong 4f–5d absorption and the corresponding emissions make Ce^{3+} ion one of the important constituents in light emitting materials.[33,34] The solid state PL spectrum of the complex was recorded using JY Horiba PL meter at room temperature with an excitation wavelength of 300 nm and the spectrum is displayed in Figure 11. The spectrum of Ce(III) shows broad emission band as the emission which result from 4f–5d transitions are generally broad. Usually, Ce^{3+} emission appears in the UV or blue spectral region.[35] Moreover, Ce(III) lacks an effective f shield and is thus influenced by the crystal field of the ligand leading to the broadening of the emission band.[36]

3.8 *Magnetic susceptibility*

The solid state room temperature magnetic susceptibility of the compound was performed on a Sherwood Scientific MK-1 magnetic susceptibility meter. In lanthanides, paramagnetism is due to the presence of 4f electrons that were effectively shielded by $5s^2 5p^6$ electrons. Moreover, the spin orbital coupling for the unpaired electrons in the f orbitals of the lanthanides is quite strong. Usually, Ce(III) complexes show effective magnetic moment in the range 2.34–2.57 BM.[37] In the case of $([Ce_2(glu)_3(H_2O)_4]\cdot 10H_2O)_n$, effective magnetic moment was calculated using the relation $\mu_{eff} = 2.828 (X_m\ T)^{1/2}$, where X_m is the molar susceptibility corrected using Pascals constants.[38] The data showed that the compound is paramagnetic with $\mu_{eff} = 2.56$ B.M..

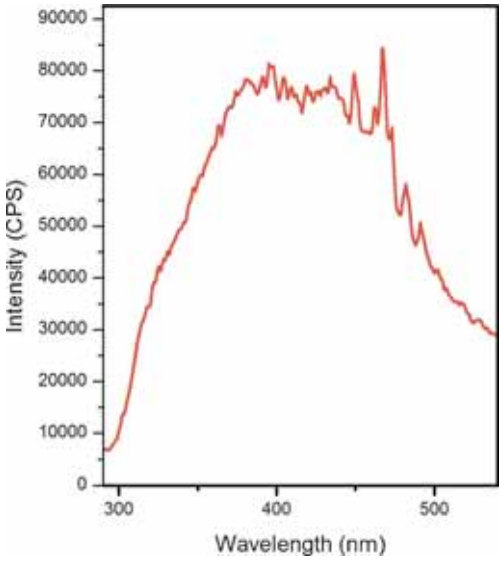

Figure 11. Room temperature solid state photoluminescence spectrum of $([Ce_2(glu)_3(H_2O)_4]\cdot 10H_2O)_n$.

4. Conclusions

A novel 2D metal–organic framework, poly[tetraaquatriglutaratodicerium(III) decahydrate] was successfully grown by single gel diffusion technique at room temperature. The crystals obtained were transparent and needle shaped. Single crystal X-ray diffraction study revealed that the compound is a porous metal–organic framework which crystallizes in orthorhombic space group *Pnma*. The metal coordination give rise to 1D chains which are further connected by glutarate ligands to form a 2D architecture. One of the important structural features of the compound is the presence of hydrophilic hexagonal channels. The stoichiometry of the compound was analyzed by elemental analysis and the molecular formula obtained, $([Ce_2(glu)_3(H_2O)_4]\cdot 10H_2O)_n$ is in accordance with single crystal X-ray diffraction results. The FT-IR spectral studies showed that the ligand is coordinated to the metal through carboxylate oxygen atom. Powder X-ray diffractogram confirmed the bulk purity and crystalline nature of the grown crystal. The thermogram showed that the compound decomposes in three stages and oxide of cerium was obtained as the final decomposition product. The optical absorption study indicated that the compound is transparent in visible region. The photoluminescence spectrum showed a broad emission band. Magnetic studies revealed paramagnetic behaviour of the complex with one unpaired electron.

Supplementary Information (SI)

CCDC 1016358 contains the supplementary crystallographic data for the compound $([Ce_2(glu)_3(H_2O)_4]\cdot 10H_2O)_n$. These data can be obtained free of charge *via* www.ccdc.cam.ac.uk/conts/retrieving.html, or from the Cambridge Crystallographic Data Centre, 12 Union Road, Cambridge CB2, 1EZ, UK; Fax: (+44) 1223-336-033, or e–mail: deposit@ccdc.cam.ac.uk. Some selected bond lengths and bond angles of the

compound (Table S1), Diamond drawing of the asymmetric unit excluding lattice water molecules (Figure S1), FT-IR spectrum (Figure S2) and check cif file are given in Supplementary Information, which are available at www.ias.ac.in/chemsci.

Acknowledgements

The authors are grateful to the authorities of Sophisticated Analytical Instrumental Facilities (SAIF), Cochin University of Science and Technology, Kochi and M G University, Kottayam for providing the instrumental facilities.We are also thankful to Dr. Shibu M Eapen, SAIF, CUSAT, Kochi for single crystal X-ray diffraction measurements. The corresponding author is grateful to the University Grants Commission (UGC) for the sanction of a minor research project (MRP(S)-0270/12-13/KLKE027/UGC-SWRO). RMN is grateful to the University of Kerala for the award of a Fellowship.

References

1. Roswell J L C and Yaghi O M 2004 *Microporous Mesoporous Mater.* **73** 3
2. Ma S and Zhou H-C 2010 *Chem. Commun.* **46** 44
3. Chouhan A, Pandey A and Mayer P 2015 *J. Chem. Sci.* **127** 1599
4. Lee J, Farha O K, Roberts J, Scheidt K A, Nguyen S T and Hupp J T 2009 *Chem. Soc. Rev.* **38** 1450
5. Nalaparaju A and Jiang J 2012 *J. Phys. Chem.* **116** 6925
6. Natarajan S, Mahata P and Sarma D 2012 *J. Chem. Sci.* **124** 339
7. Gandara F, de Andres A, Gomez-Lor B, Gutierrez-Puebla E, Iglesias M, Monge M A, Prosperpio D M and Snejko N 2008 *Cryst. Growth Des.* **8** 378
8. Perles J, Iglesias M, Ruiz-Valero C and Snejko N 2004 *J. Mater. Chem.* **14** 2683
9. Cao X, Yu L and Huang R 2014 *J. Solid State Chem.* **210** 74
10. Chen Y and Ma S 2012 *Rev. Inorg. Chem.* **32** 81
11. Rocha J, Carlos L D, Almeida Paz F A and Ananias D 2011 *Chem. Soc. Rev.* **40** 926
12. Anoop M R, Binil P S, Suma S and Sudarsanakumar M R 2012 *J. Rare Earths* **30** 709
13. Huang W, Wu D, Zhou P, Yan W B, Guo D, Duan C Y and Meng Q J 2009 *Cryst. Growth Des.* **9** 1361
14. Sun J and Zheng Y-Q 2003 *Z. Anorg. Allg. Chem.* **629** 1001
15. Lee E W, Kim Y J and Jung D-Y 2002 *Inorg. Chem.* **41** 501
16. Rao C N R, Natarajan S and Vaidhyanathan R 2004 *Angew. Chem. Int. Ed.* **43** 1466
17. Ren Y P, Long L S, Mao B W, Yuan Y Z, Huang R B and Zheng L S 2003 *Angew. Chem. Int. Ed.* **42** 532
18. Aliouane K, Djeghri A, Guehria-Laidoudi A, Dahaoui S and Lecomte C 2007 *J. Mol. Struct.* **832** 150
19. Rahahlia N, Benmerad B, Guehria-Laidoudi A, Dahaoui S and Lecomte C 2006 *Acta Cryst. E* **62** 2145
20. Roy S M, Sudarsanakumar M R, Suma S, Kurup M R P and Dhanya V S 2013 *J. Inorg. Organomet. P.* **23** 608
21. Nair R M, Sudarsanakumar M R, Suma S, Kurup M R P and Antarjanam P K S 2016 *Inorg. Chem. Commun.* **63** 81
22. Nair R M, Sudarsanakumar M R, Suma S and Kurup M R P 2016 *J. Mol. Struct.* **1105** 316
23. *APEXII and SAINT* 2004 (Bruker AXS: Madison, WI)
24. Sheldrick G M 1997 In *SHELXL 97 Program for Crystal Structure Refinement* (Gottingen, Germany: University of Gottingen)
25. Brandenburg K 2008 In *DIAMOND Version 3.1f* (Bonn: Crystal Impact, GbR)
26. Bruno I J, Cole J C, Edgington P R, Kessler M, Macrae C F, McCabe P, Pearson J and Taylor R 2002 *Acta. Cryst.* **58B** 389
27. Oh Y, Kim J Y, Kim H J, Lee T and Kang S W 2010 *Bull. Kor. Chem. Soc.* **31** 1058
28. Millward A R and Yaghi O M 2005 *J. Am. Chem. Soc.* **127** 17998
29. Ma S 2009 *Pure Appl. Chem.* **81** 2235
30. Mitra T, Sailakshmi G and Gnanamani A 2014 *J. Chem. Sci.* **126** 127
31. Hou K-L, Bai F-Y, Xing Y-H, Wang J-L and Shi Z 2011 *Inorg. Chim. Acta* **365** 269
32. Vogler A and Kunkely H 2006 *Inorg. Chim. Acta* **359** 4130
33. Trusova E E, Bobkova N M, Gurin V S and Tyavlovskaya E A 2006 *Glass Ceram.* **66** 7
34. Prokhorova T I and Ostrogina O M 1981 *Fiz. Khim. Stekla* **7** 678
35. Blasse G and Brill A 1967 *J. Chem. Phys.* **47** 5139
36. de Oliveira C A F, da Silva F F, Malvestiti I, Malta V R S, Dutra J D L, da Costa Jr. N B, Freire R O and Alves S 2013 *J. Mol. Struct.* **1041** 61
37. El-Wahab Z H A, Mashaly M M and Faheim A A 2005 *Chem. Pap. - Chem. Zvesti* **35** 25
38. Gordon A B and John F B J 2008 *Chem. Edn.* **85** 532